Polar Angle as a Determinant of Amphipathic α-Helix-Lipid Interactions: A Model Peptide Study

Natsuko Uematsu* and Katsumi Matsuzaki†
*Graduate School of Pharmaceutical Sciences and †Graduate School of Biostudies, Kyoto University, Kyoto 606-8501, Japan

ABSTRACT Various physicochemical properties play important roles in the membrane activities of amphipathic antimicrobial peptides. To examine the effects of the polar angle, two model peptides, θp100 and θp180, with polar angles of 100° and 180°, respectively, were designed, and their interactions with membranes were investigated in detail. These peptides have almost identical physicochemical properties except for polar angle. Like naturally occurring peptides, these peptides selectively bind to acidic membranes, assuming amphipathic α-helices, and formed peptide-lipid supramolecular complex pores accompanied by lipid flip-flop and peptide translocation. Despite its somewhat lower membrane affinity, θp100 exhibited higher membrane permeabilization activity, a greater flip-flop rate, as well as more antimicrobial activity due to a higher pore formation rate compared with θp180. Consistent with these results, the peptide translocation rate of θp100 was higher. Furthermore, the number of peptides constituting θp100 pores was less than that of θp180, and θp100 pores involved more lipid molecules, as reflected by its cation selectivity. The polar angle was found to be an important parameter determining peptide-lipid interactions.

INTRODUCTION

Recently, the appearance of bacteria resistant to conventional antibiotics has become a serious medical problem. Therefore, the development of antibiotics with novel mechanisms of action is an urgent issue. Endogenous antimicrobial peptides such as magainin 2 (Zasloff, 1987; Matsuzaki, 1998, 1999) and PGLa (Hoffmann et al., 1983; Matsuzaki et al., 1998a), isolated from the skin of the African clawed frog *Xenopus laevis*, are promising candidates (Matsuzaki, 1998, 1999). The cationic amphipathic α-helix is a common structural motif of many antimicrobial peptides (Epand et al., 1995). These peptides selectively interact with negatively charged bacterial membranes by electrostatic interaction and exert antimicrobial activity by permeabilizing cell membranes. Many attempts have been made to design new antimicrobial drugs for clinical use (Hancock, 1999), including studies of the structure-activity relationships of naturally occurring peptides (Maloy and Kari, 1995) and the de novo design of amphipathic model peptides exclusively composed of Lys, Leu, Ala, and Gly (Blondelle and Houghten, 1992; Javadpour and Juban, 1996).

Various mechanisms, such as formation of ion channels and disturbance of lipid bilayers, have been suggested to be involved in membrane permeabilization by these antimicrobial peptides (Hancock et al., 1995; Bechinger, 1999). The following mechanism of action was proposed in our laboratory for magainin 2 and PGLa. Several helices form a dynamic peptide-lipid supramolecular complex pore, which allows not only ion transport but also a rapid flip-flop of membrane lipids (Matsuzaki et al., 1996a). Upon disintegration of the pore, a fraction of the peptide molecules stochastically translocate into the inner leaflet (Matsuzaki et al., 1995a,b). This mechanism is also applicable to another venom peptide, mastoparan X (Matsuzaki et al., 1996b). On the other hand, model peptides were suggested to permeabilize lipid bilayers by phase separation or disruption of lipid organization (Dathe et al., 1996).

Because peptide-induced membrane permeabilization is a consequence of physicochemical interactions between peptides and lipids, the physicochemical parameters of peptides such as charge, hydrophobicity (H), hydrophobic moment (μ), helicity, and the angle subtended by the polar face (θ_p) of the amphipathic α-helix should modulate the mode of action, pore formation rate, pore stability, etc. Elucidation of the effects of these parameters is crucial for the development of potent peptidic antibiotics. For example, magainin 2 and PGLa apparently exhibit very similar membrane permeabilization activities. However, the former is characterized by slow pore formation and high pore stability, whereas the latter shows fast pore formation and low pore stability (Matsuzaki et al., 1998). The physicochemical properties of magainin 2 and PGLa are quite different. Each of these parameters is considered to affect the peptide-membrane interactions differently, but their individual influences have not been clarified in detail. Among these properties, little information is available about the effects of θ_p compared to charge (Matsuzaki et al., 1997a), H (Matsuzaki et al., 1995c; Wieprecht et al., 1997b; Dathe et al., 1997), helicity (Dathe et al., 1996),and μ (Wieprecht et al., 1997a; Dathe et al., 1997). The only information available is that a decrease in θ_p increases the apparent membrane permeabilization (Wieprecht et al., 1997c; Dathe et al., 1997).

In this study, two amphipathic model peptides, θp100 and θp180, with θp values of 100° and 180°, respectively, were synthesized de novo while the other physicochemical pa-

Received for publication 27 March 2000 and in final form 16 June 2000.
Address reprint requests to Dr. Katsumi Matsuzaki, Graduate School of Biostudies, Kyoto University, Sakyo-ku, Kyoto 606-8501, Japan. Tel.: 81-75-753-4574; Fax: 81-75-761-2698; E-mail: katsumim@pharm.kyoto-u.ac.jp.

0006-3495/00/10/2075/09 $2.00

rameters were kept almost identical. We found that these simple model peptides also followed a supramolecular pore formation-translocation scheme similar to that of magainin 2. A decrease in θp markedly enhanced the pore formation rate and reduced pore stability, therefore increasing translocation ability. The overall membrane-permeabilizing activity of θp100 was greater than that of θp180. Furthermore, θp100 formed pores involving more lipid molecules, facilitating more efficient lipid flip-flop. This was also reflected in the ion selectivity of the pores. Thus we elucidated a change in the single physicochemical parameter that can have drastic effects on peptide-lipid interactions.

MATERIALS AND METHODS

Materials

The model peptides were synthesized by a fluoren-9-ylmethoxycarbonyl-based solid-phase method and purified by reverse-phase high-performance liquid chromatography (RP-HPLC) and gel filtration as previously described (Matsuzaki et al., 1991, 1994). The purities of the synthesized peptides were determined by RP-HPLC and ion spray mass spectroscopy. *N*-[[(5-(Dimethylamino)naphthyl]-1-sulfonyl] egg yolk L-α-phosphatidylethanolamine (DNS-PE) and 1-palmitoyl-2-[6-((7-nitrobenz-2-oxa-1,3-diazol-4-yl)amino)caproyl]-L-α-phosphatidylcholine (C_6-NBD-PC) were purchased from Avanti Polar Lipids (Alabaster, AL). The other phospholipids, phosphate-buffered saline and fluorescein isothiocyanate-dextran of MW 4400 (FITC-dextran) were obtained from Sigma (St. Louis, MO). Calcein and spectrograde organic solvents were supplied by Dojindo (Kumamoto, Japan). 8-Aminonaphthalene-1,3,6-trisulfonic acid (ANTS) and *p*-xylene-bis-pyridinium bromide (DPX) were obtained from Molecular Probes (Eugene, OR). All other chemicals, obtained from Wako (Tokyo, Japan), were of special grade. Tris-HCl buffer (10 mM Tris, 150 mM NaCl, 1 mM EDTA, pH 7.4) was prepared from Nanopure water (Barnstead).

Vesicle preparation

Large unilamellar vesicles (LUVs) were prepared and characterized as described elsewhere (Matsuzaki et al., 1996a). Briefly, a lipid film, after drying under vacuum overnight, was hydrated with the buffer or the solution used for each experiment and vortex-mixed to produce multilamellar vesicles (MLVs). The suspension was subjected to five or 10 freeze-thawed cycles and then extruded through polycarbonate filters (two stacked 0.1-μm pore size filters, 10 times). Small unilamellar vesicles (SUVs) for circular dichroism (CD) measurements were produced by sonication of the freeze-thawed MLVs in ice water under a nitrogen atmosphere. The lipid concentration was determined in triplicate by phosphorus analysis (Bartlett, 1959).

CD spectra

CD spectra were measured on a Jasco J-720 apparatus connected to an NEC PC-9801 microcomputer, using a 1-mm path length quartz cell to minimize the absorbance due to buffer components. The instrumental outputs were calibrated with nonhygroscopic ammonium *d*-camphor-10-sulfonate (Takakuwa et al., 1985). Eight scans were averaged for each sample, and the average blank spectra were subtracted. The peptide concentration was 25 μM. The absence of any optical artifacts was confirmed as described elsewhere (Matsuzaki et al., 1989).

Calcein leakage

Membrane-permeabilizing activity was detected by calcein leakage (Matsuzaki et al., 1998a). LUVs containing 70 mM calcein and calcein-free LUVs were mixed to obtain the desired lipid concentration. The release of calcein from the LUVs was fluorometrically monitored at an excitation wavelength of 490 nm and an emission wavelength of 520 nm. The maximum fluorescence intensity corresponding to 100% leakage was determined by the addition of 10% (w/v) Triton X-100 (20 μl) to the sample (2 ml). The apparent percent leakage value was calculated according to Eq. 1. F and F_t denote, respectively, the fluorescence intensity before and after the addition of detergent:

$$\%\ \text{apparent leakage} = 100(F - F_0)/(F_t - F_0) \quad (1)$$

F_0 represents the fluorescence intensity of intact vesicles.

FITC-dextran leakage

A double-labeling method developed by our laboratory was utilized (Matsuzaki et al., 1997c). LUVs composed of egg yolk L-α-phosphatidyl-D,L-glycerol (PG)/egg yolk L-α-phosphatidylcholine (PC)/DNS-PE (65.2:33.3:1.5) entrapping 20 mM FITC-dextran (MW4400) were incubated with the peptide for 5 min. A 48 mg/ml trypsin solution (20 μl) was added to stop membrane permeabilization. The leaked FITC-dextran was removed by gel filtration (Bio-Gel, A-1.5m). The excitation spectrum of the vesicle fraction after solubilization with Triton X-100 was measured at an emission wavelength of 520 nm. The percent leakage value was calculated as reported elsewhere (Matsuzaki et al., 1997c).

Pore lifetime and pore formation rate

The pore lifetime, τ, can be evaluated by the extent of self-quenching of the peptide-treated, calcein-entrapped PG/PC (2:1) LUVs (Schwarz and Arbuzova, 1995; Matsuzaki et al., 1998a). After calcein-containing LUVs were mixed with the peptide, the time course of changes in calcein fluorescence was monitored. Immediately after the apparent percent leakage value reached 60–80%, 20 μl of trypsin solution (48 mg/ml) was added to stop leakage completely. The liposome suspension (250 μl) was immediately sampled. Triton X-100 was added to the rest of the liposome suspension. The apparent retention, E, was calculated according to Eq. 2:

$$E = (F_t - F)/(F_t - F_0) \quad (2)$$

The sampled liposomes were applied to a Bio-Gel A-1.5m column to separate the vesicle fraction from leaked calcein, and its quenching factor (Q) was obtained by measuring the fluorescence intensity before (F_b) and after (F_a) the addition of Triton X-100:

$$Q = F_b/F_a \quad (3)$$

The Q value was plotted against the E value. The ρ value, a dimensionless parameter introduced by Schwarz and Arbuzova to describe the pore life span (Schwarz and Arbuzova, 1995), was estimated from theoretical Q versus E curves for various ρ values:

$$\rho = \tau_0/(\tau + \tau_0) \quad (4)$$

τ_0 is the time necessary for a $1/e$ reduction of the intravesicular dye concentration. The number of calcein-permeable pores formed per vesicle, p, was calculated according to Eq. 5:

$$p = -(\ln R)/(1 - \rho) \quad (5)$$

The true retention of the dye, R, was obtained from the apparent retention, E, by the method of Schwarz and Arbuzova (1995).

Flip-flop

The peptide-induced lipid flip-flop was determined as previously reported (Matsuzaki et al., 1996a, 1998). 7-Nitrobenz-2-oxa-1,3-diazol-4-yl (NBD)-labeled LUVs composed of PG and PC (2:1) containing 0.5 mol% C_6-NBD-PC were mixed with 1 M sodium dithionite/1 M Tris ([lipid] = 8 mM, [dithionite] = 60 mM) and incubated for 15 min at 30°C to produce inner leaflet-labeled vesicles. The vesicles were immediately separated from dithionite by gel filtration. The asymmetrically NBD-labeled LUVs were incubated with or without the peptide for various periods at 30°C. The fraction of NBD-lipids that had flopped during incubation was measured on the basis of fluorescence quenching by sodium dithionite. After the addition of trypsin solution (48 mg/ml) to recover the membrane barrier, 20 μl of 1 M sodium dithionite/1 M Tris solution was added. Fluorescence was monitored at excitation and emission wavelengths of 460 and 530 nm, respectively. The percentage flip-flop value was calculated as described previously (Matsuzaki et al., 1996a).

Peptide binding and translocation

Resonance energy transfer (RET) from the Trp residue to the dansyl chromophore was utilized to monitor the peptide-membrane association. LUVs composed of PG/PC/DNS-PE (61.7:33.3:5) were added to the peptide solution, and sensitized dansyl fluorescence was monitored at an excitation wavelength of 285 nm and an emission wavelength of 512 nm. For the detection of translocation, 200 μM trypsin was encapsulated within LUVs. The enzyme outside the vesicles was inactivated by the addition of a fourfold excess of trypsin inhibitor. Peptide translocation was observed as a decrease in dansyl fluorescence because trypsin-digested peptide fragments were desorbed from the membrane. As a control, LUVs containing 200 μM trypsin and 800 μM trypsin inhibitor were also prepared. The difference in dansyl fluorescence between the two types of LUVs gives a measure of the extent of peptide translocation.

ANTS/DPX leakage

ANTS-DPX leakage mode and selectivity were estimated by the fluorescence requenching procedure (Ladokhin et al., 1995; Wimley et al., 1994). PG/PC (2:1) LUVs entrapping 6 mM ANTS and 24 mM DPX were disrupted with Triton X-100, and ANTS fluorescence (F_{max}) was monitored at an excitation wavelength of 353 nm and an emission wavelength of 520 nm. After the addition of various amounts (final concentrations 0.5–5 mM) of DPX, fluorescence (F_{DPX}) was again measured. Quenching outside values (Q_{out}) were obtained as a function of DPX concentration:

$$Q_{out}([DPX]) = F_{DPX}([DPX])/F_{max} \quad (6)$$

The total quenching values (Q_{total}) were then determined as follows. After LUVs were incubated with peptide solutions for various periods (Δ), 20 μl of trypsin solution (48 mg/ml) was added to 2 ml of sample to stop dye leakage. The final peptide and lipid concentrations were 1.5 and 45 μM for θp100 and 3.9 and 40 μM for θp180. Various amounts of DPX were added, and the fluorescence was measured (F_{total}). The addition of Triton X-100 yielded F_{DPX} values. The F_{max} value for each DPX concentration was obtained using Eq. 6. Total quenching (Q_{total}) is defined by

$$Q_{total}([DPX], \Delta) = F_{total}([DPX], \Delta)/F_{max} \quad (7)$$

By plotting Q_{total} against Q_{out} for each Δ, the fractions of ANTS outside (f_{out}) and quenching inside (Q_{in}) were estimated from Eq. 8:

$$Q_{total}([DPX], \Delta) = Q_{out}([DPX], \Delta) \cdot f_{out}(\Delta) + Q_{in}(\Delta) \cdot [1 - f_{out}(\Delta)] \quad (8)$$

All of the spectroscopic measurements were carried out at 30°C.

Antibacterial activity and hemolytic activity

The minimum inhibitory concentration (MIC) values of the peptides against *Escherichia coli* (ATCC 8739) were determined as previously described (Matsuzaki et al., 1994). Briefly, bacterial cells (10^6 cfu/ml) in the midlogarithmic growth phase were incubated with various concentrations of sterilized peptides (6.25, 12.5, 25, 50, 100, 200, and 400 μM) in the presence of nutrients for 8 h at 37°C. Bacterial growth was determined from the optical density at 405 nm.

The hemolytic activities of the peptides were determined using fresh human erythrocytes (blood type O). The blood was centrifuged and washed three times with phosphate-buffered saline to remove the plasma and buffy coat. Peptide solutions were incubated with an erythrocyte suspension (final erythrocyte concentration, 1% v/v) at 37°C for 1 h. The percentage hemolysis was determined from the optical density at 540 nm of the supernatant after centrifugation (2000 × *g*, 10 min). Hypotonically lysed erythrocytes were used as a standard for 100% hemolysis.

RESULTS

Peptide design

To evaluate the effects of the polar angle of amphipathic antimicrobial peptides on membrane, antimicrobial, and hemolytic activities, two amphipathic model peptides, designated as θp100 and θp180, were designed. Fig. 1 shows the amino acid sequences and the helical wheel representations of these model peptides. The peptides were exclusively composed of helix-promoting Lys, Ala, Leu, and Trp. Trp was introduced to monitor peptide-membrane interactions. The fluorophore was located at the hydrophobic-hydrophilic interface because Trp tends to seek the membrane surface (Deisenhofer and Michel, 1989; Landolt-Marticorena et al., 1993). The polar angles of θp100 and θp180 are ~100° and ~180°, corresponding to those of PGLa (100°) and ma-

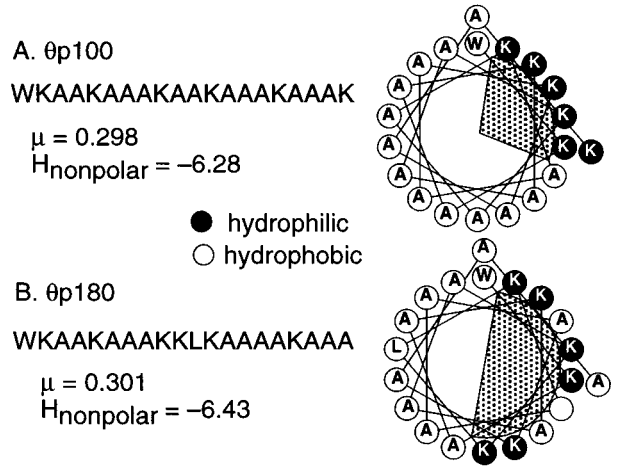

FIGURE 1 The amino acid sequences and helical wheel representations of (*A*) θp100 and (*B*) θp180. The shaded area indicates the hydrophilic surface of the amphipathic helix. The hydrophobic moment (μ) and the hydrophobicity of the helix nonpolar face ($H_{nonpolar}$) were calculated from the free energies (kcal/mol) of transfer of *N*-acetyl amino acid amides from water to 1-octanol (Fauchère and Pliška, 1983).

gainin 2 (180°), respectively. Both peptides have a +6 charge originating from six lysine residues for potent antimicrobial activities (Matsuzaki et al., 1997b) and almost the same μ values, hydrophobicities of the nonpolar faces ($H_{nonpolar}$), and amino acid compositions. The hydrophobicities are low to avoid toxicity against erythrocytes (Matsuzaki et al., 1995c). Therefore, differences in peptide activity should clearly reflect the effects of polar angle.

CD

The secondary structures of the peptides were estimated by CD. Fig. 2 shows CD spectra of θp100 under various conditions, and those of θp180 were almost identical (data not shown). Both peptides adopted unordered structures in buffer and even in the presence of zwitterionic PC membranes, indicating that these peptides do not bind to PC. In contrast, the peptides bound to acidic PG/PC (2:1) bilayers, forming α-helical structures as characterized by double minima at 208 and 222 nm.

Membrane permeabilization and biological activity

Membrane-permeabilizing activity was examined on the basis of the efflux of the anionic, fluorescent dye calcein from LUVs of various lipid compositions. Fig. 3 shows the apparent percent leakage value at 5 min as a function of the peptide-to-lipid molar ratio (P/L). The lytic activity of θp100 against PG/PC (2:1) membranes was ~2.3-fold higher than that of θp180. Both peptides were inactive against zwitterionic PC membranes, which is consistent with the CD data (Fig. 2). In addition, replacement of PC in PG/PC (2:1) membranes by negative curvature-inducing egg yolk L-α-phosphatidylethanolamine (PE) greatly reduced the activities of both peptides. In these experiments, addition of the peptides induced neither membrane aggregation nor micellization, as confirmed by right-angle light scattering (data not shown).

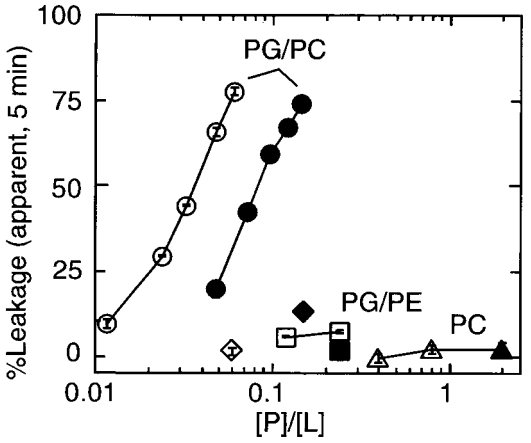

FIGURE 3 The effects of lipid composition on the membrane permeabilization by θp100 (○, □, ◇, △) and θp180 (●, ■, ◆, ▲). The apparent percent leakage values of calcein from PG/PC (2:1) LUVs (○, ●), PG/PE (2:1) LUVs (□, ■) and PC LUVs (△, ▲) during a 5-min period are plotted as a function of P/L. ◇, ◆, Percentage leakage values of FITC-dextran from PG/PC (2:1) LUVs.

Fig. 4 demonstrates that the antimicrobial activity of θp100 against *E. coli* (MIC ~200 μM) was again threefold higher than that of θp180 (MIC ~600 μM by extrapolation). Neither peptide showed any measurable hemolytic activity (<3%) at a concentration of 0.9 mM, whereas PGLa exhibited 42% hemolysis.

Pore properties

To evaluate pore size, extents of release of three dyes of different sizes, i.e., ANTS (MW 427), calcein (MW 623),

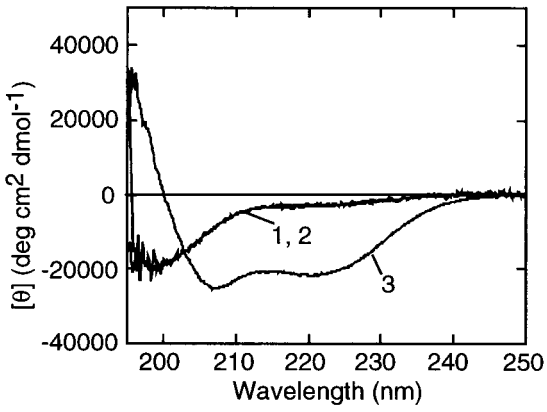

FIGURE 2 CD spectra of θp100 measured at 30°C ([peptide] = 25 μM). Spectra in Tris buffer (10 mM Tris, 150 mM NaCl, 1 mM EDTA, pH 7.4) in the presence of 2 mM PC SUVs and 1.6 mM PG SUVs are represented by traces 1, 2, and 3, respectively.

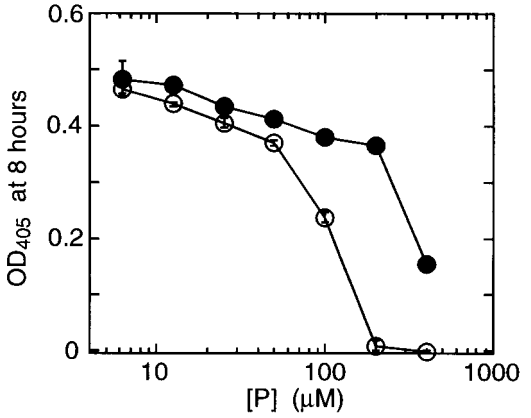

FIGURE 4 Antimicrobial activities. The peptides were mixed with *E. coli* cells (10^6 cfu/ml). Optical density at 405 nm after an 8-h incubation at 37°C is plotted as a function of peptide concentration. ○, θp100; ●, θp180.

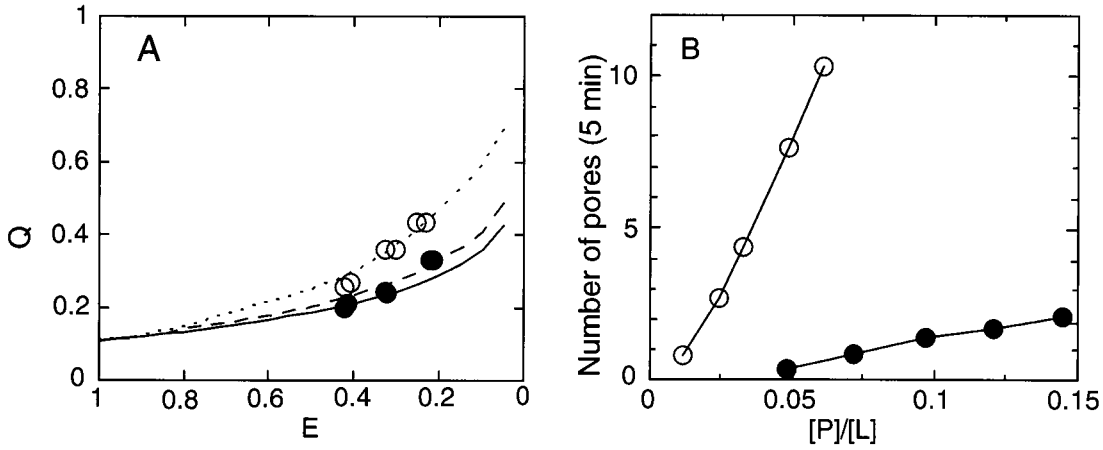

FIGURE 5 (*A*) Estimation of pore lifetime at 30°C. The apparent retention, *E*, is shown against the quenching factor, *Q*. Peptides: ○, θp100; ●, θp180. Theoretical curves for $\rho = 0.4$ (——), 0.5 (– – –), and 0.9 (·····) calculated according to the method of Schwarz and Arbuzova (1995) are also shown. (*B*) The number of pores formed during a 5-min incubation was calculated from the dose-response curves for calcein release and the pore lifetime according to Eq. 5. Peptides: ○, θp100; ●, θp180.

and FITC-dextran (MW 4400), were compared. Fig. 3 (*diamonds*) shows that FITC-dextran was slightly permeable through θp180 pores, whereas the dye could not pass through θp100 pores under the conditions at which 80% calcein leakage was observed. The leakage of ANTS occurred in the same range of peptide concentration as that of calcein (data not shown).

Pore lifetime was estimated on the basis of self-quenching of calcein according to the method of Schwarz and Arbuzova (1995). The quenching factor (Q) of calcein is plotted against apparent retention (E) in Fig. 5 *A*. Comparison of the data with theoretical curves estimated ρ values of θp100 and θp180 to be 0.9 and 0.45 (± 0.1), respectively, corresponding to $\tau = 0.1\tau_0$ and $1.2\tau_0$. That is, the pore lifetime of θp100 was 12-fold shorter than that of θp180, assuming the τ_0 values of the two peptides were the same (see Discussion). The number of calcein-permeable pores formed per vesicle, p, during a 5-min period is plotted as a function of P/L in Fig. 5 *B*. θp100 was found to exhibit a higher membrane-permeabilizing activity than θp180 (Fig. 3) by forming pores much more frequently (Fig. 5 *B*), compensating for the short pore lifetime.

Furthermore, we evaluated the ANTS/DPX leak mode and selectivity. The quenching inside value (Q_{in}) was plotted against the fraction of ANTS outside value (f_{out}) in Fig. 6. Based on a comparison of theoretical Q_{in} versus f_{out} curves with the data (Ladokhin et al., 1995), we estimated the α values to be 9 and 1 for θp100 and θp180, respectively. The ratio of the release rate of DPX to that of ANTS is denoted by α. That is, θp100 induced DPX (cation)-selective, graded mode leakage, whereas θp180 induced nonselective, graded mode leakage.

Peptide binding

Fig. 7 shows that addition of dansyl-labeled LUVs to a peptide solution at time 0 caused a dose-dependent increase in dansyl fluorescence, indicating RET due to the binding of the peptide to the membrane. The binding reaction was time-dependent and biphasic, i.e., fast initial binding following by slow additional binding. The latter process was pronounced at higher peptide concentrations. These results suggested that peptides once bound to the outer leaflets translocated into the inner leaflets, so that free peptides could further bind to the less populated outer leaflets. Comparison of the initial values at [P] = 2 μM revealed that the

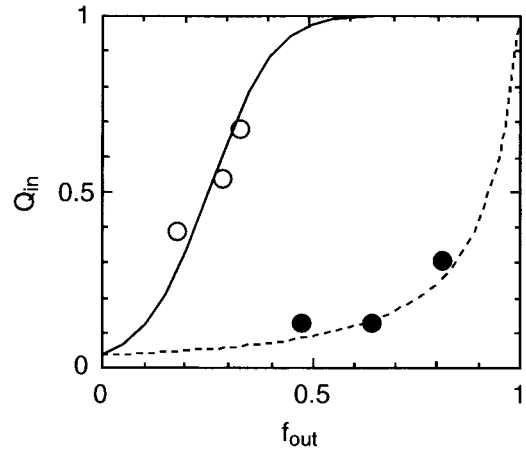

FIGURE 6 Estimation of ion selectivity. Intravesicular quenching of ANTS (Q_{in}) is plotted as a function of the released fraction of ANTS (f_{out}) for leakage induced by θp100 (○) and θp180 (●). Theoretical curves for $\alpha = 9$ and 1 are shown by the solid and broken traces, respectively. See text for details.

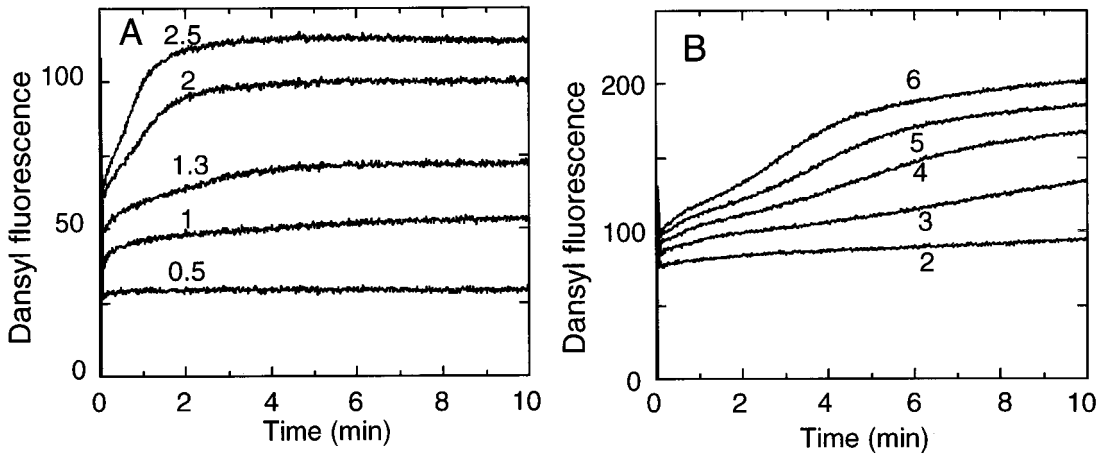

FIGURE 7 Time-dependent peptide binding. Peptide binding was evaluated by the use of RET from the Trp residues to DNS-PE. (*A*) Binding of θp100. The peptide concentrations were 2.5, 2, 1.3, 1 and 0.5 μM from top to bottom. (*B*) Binding of θp180. The peptide concentrations were 6, 5, 4, 3 and 2 μM from top to bottom. The lipid concentration was 41.5 μM.

binding affinity of θp180 was slightly higher than that of θp100.

To exclude the possibility that the biphasic binding is caused by decelerated binding due to complete charge neutralization, we measured binding directly. The lipid film was hydrated with the peptide solution and vortex-mixed. After ultracentrifugation, the free peptide concentration was determined fluorometrically. At [θp100] = 2.5 μM and [lipid] = 41.5 μM, the free peptide concentration was 1 μM, corresponding to only ~30% charge neutralization.

Peptide translocation and lipid flip-flop

Translocation of the peptide across lipid bilayers was detected on the basis of digestion of translocated peptides by trypsin entrapped within the vesicles (Matsuzaki et al., 1995a). The extent of peptide translocation relative to the amount of initially bound peptides is shown in Fig. 8. We chose peptide concentrations showing almost the same extent (~70%) of calcein leakage (Fig. 3). The rate of translocation of θp100 was greater than that of θp180, although the concentration of θp100 was significantly lower. Fig. 9 shows that the rate of lipid flip-flop induced by θp100 was again larger than that of θp180.

DISCUSSION

Biological activities

For low hemolytic activity, the peptides were designed to possess alanine residues with low hydrophobicity. The surface of the mammalian cell membrane is exclusively composed of electrically neutral zwitterionic phospholipids, for which the peptide's affinity is governed by hydrophobic interactions. As expected, θp100 and θp180 did not show any detectable hemolysis at a peptide concentration as high as 0.9 mM, consistent with the observation that the peptides do not permeabilize PC bilayers (Fig. 3). In contrast, magainin 2 (Matsuzaki et al., 1997b) and PGLa, with greater hydrophobicities ($H_{\text{nonpolar}} = -9.61$ and -12.16 kcal/mol, respectively), exhibited 40–50% hemolysis under similar conditions. For potent antimicrobial activity, six positive charges were introduced into the model peptides (Matsuzaki et al., 1997b). Bacterial membranes are abundant in acidic lipids, which attract basic peptides. A large positive charge is especially effective for permeabilizing the outer membranes of Gram-negative bacteria (Matsuzaki et al., 1997b). The model peptides permeabilized negatively charged

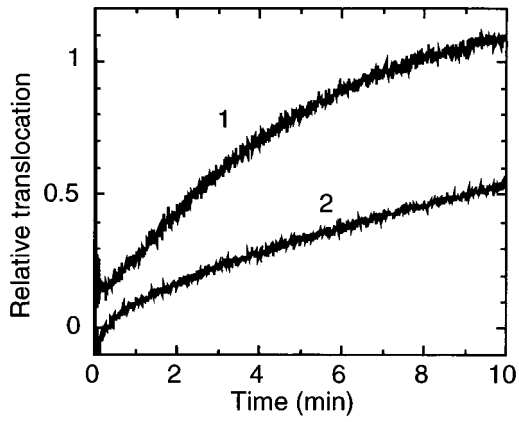

FIGURE 8 Detection of peptide translocation. The peptides were mixed with trypsin-encapsulating LUVs (41.5 μM) composed of PG/PC/DNS-PE (61.7:33.3:5). The enzyme digested the translocated peptides, desorbing the fragments off the bilayers. The extent of translocation relative to the amount of initially bound peptides was evaluated by the decrease in sensitized dansyl fluorescence. Peptide: curve 1, θp100 (2 μM); curve 2, θp180 (5 μM).

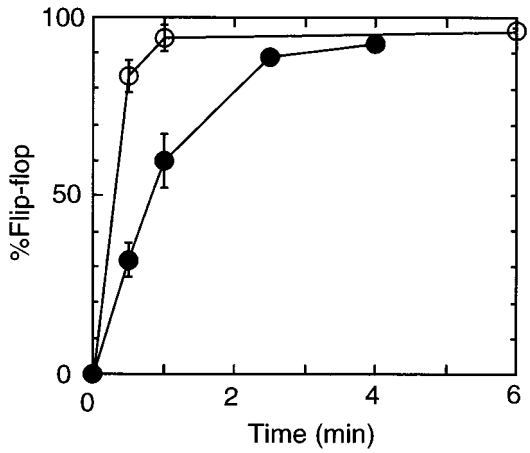

FIGURE 9 Peptide-induced flip-flop of membrane lipids. Time courses of changes in percentage of flip-flop are shown for θp100 (○) and θp180 (●). The peptide concentrations were 2 μM for θp100 and 5 μM for θp180. The lipid concentration was 50 μM.

PG/PC bilayers. θp100 was more active (Fig. 3), in accordance with its higher antimicrobial activity (Fig. 4). For magainin analogs, a decrease in θp also enhanced the permeability of model membranes (Wieprecht et al., 1997c). However, no clear correlation was observed between θp and MIC for magainins and model peptides (Wieprecht et al., 1997c; Dathe et al., 1997). The antimicrobial activities of our model peptides (MIC 200–600 μM) were much lower than those of magainin 2 and PGLa (MIC 50 μM) because electrostatic interactions alone are not large enough for these peptides with extremely low hydrophobicities (Fig. 1) to achieve complete binding to negatively charged membranes (Fig. 7).

The binding affinity of θp180 for PG/PC bilayers was slightly larger than that of θp100 (Fig. 7). The total hydrophobicity of Leu-containing θp180 was larger than that of θp100, although the H_{nonpolar} values were very similar (Fig. 1). The Ala residues in the polar face of θp180 may make a slight contribution to the binding affinity. The affinity of the magainin analog with $\theta p = 180$ was an order of magnitude greater than that of the analog with $\theta p = 100$ (Wieprecht et al., 1997c). These two peptides have similar total hydrophobicities but different H_{nonpolar} values. Therefore, the H_{nonpolar} value appears to be a parameter more relevant to binding affinity.

Mechanism of membrane permeabilization

Several mechanisms have been proposed for peptide-induced membrane permeabilization (Hancock et al., 1995; Bechinger, 1999). The dynamic, peptide-lipid supramolecular complex pore model was proposed to explain mutually coupled dye leakage and lipid flip-flop (Matsuzaki et al., 1996a). It should be noted that some investigators use the term "pore" to describe a channel-like hole with a well-defined structure, whereas others take the word in a broader sense. The characteristics of our pore are as follows. The pore has a measurable mean lifetime (Fig. 5 *A*), size limit (Fig. 3), and ion selectivity (Fig. 6). These observations suggest that the average structure of the pore is better defined than mere membrane defects. However, it is highly probable that the pore is heterogeneous, because the numbers of peptides as well as lipids constituting a pore vary pore by pore. Even in the case of channel-forming alamethicin, one observes an ensemble of different aggregates at a certain peptide-to-lipid ratio. Nevertheless, the possibility of other mechanisms, e.g., the in-plane diffusion model (Bechinger, 1999), cannot be excluded because there is no direct observation of the pore structure.

Although the interactions of various model peptides with membranes have been investigated, it is not clear whether model peptides with simple sequences also form peptide-lipid supramolecular complex pores (Dathe et al., 1996, 1997; Blondelle and Houghten, 1992; Javadpour and Juban, 1996). The following observations clearly showed that the model peptides θp100 and θp180 formed supramolecular complex pores in a manner similar to that of the pore formation of naturally occurring peptides such as magainin 2 and PGLa: 1) The peptides induce flip-flop of lipids (Fig. 9) and translocate into the inner leaflets (Fig. 8) under conditions in which leakage occurred (Fig. 3). 2) The leakage activities were greatly reduced against liposomes containing PE, which induces negative curvature strain on the membrane (Fig. 3). Peptide-induced positive curvature in the membrane in the direction along the helical axis, which is antagonized by PE, facilitates the formation of toroidal pores (Matsuzaki et al., 1998b). Unlike magainin 2 and PGLa (Matsuzaki et al., 1998a), θp100 and θp180 did not exhibit synergism (data not shown), corroborating the hypothesis that magainin 2 and PGLa show synergism by a molecular recognition mechanism.

Characterization of pores

At P/L values at which the extent of calcein leakage was ~80%, θp100 and θp180 induced, respectively, 0 and 12% FITC-dextran leakage. The dimensions of FITC-dextran as an oblate ellipsoid are ~2 nm × ~4 nm, whereas those of calcein are 1 nm × 2 nm. Therefore, the diameter of θp100 pores was ~2–3 nm and that of θp180 pores was somewhat larger. Simple calculations suggested that θp180 pores are not large enough (≤4 nm) for free leakage of FITC-dextran. According to Schwarz and Robert (1990), the leakage of a dye obeys first-order kinetics:

$$\ln R = -t/\tau_0 \propto -A_p\, t/r \qquad (9)$$

with A_p and r representing the effective cross section of the pore and the radius of the dye, respectively. With an FITC-dextran/calcein radii ratio of ~2, Eq. 9 predicts R (FITC-dextran) ≈ (R (calcein))$^{1/2}$. However, the observed R

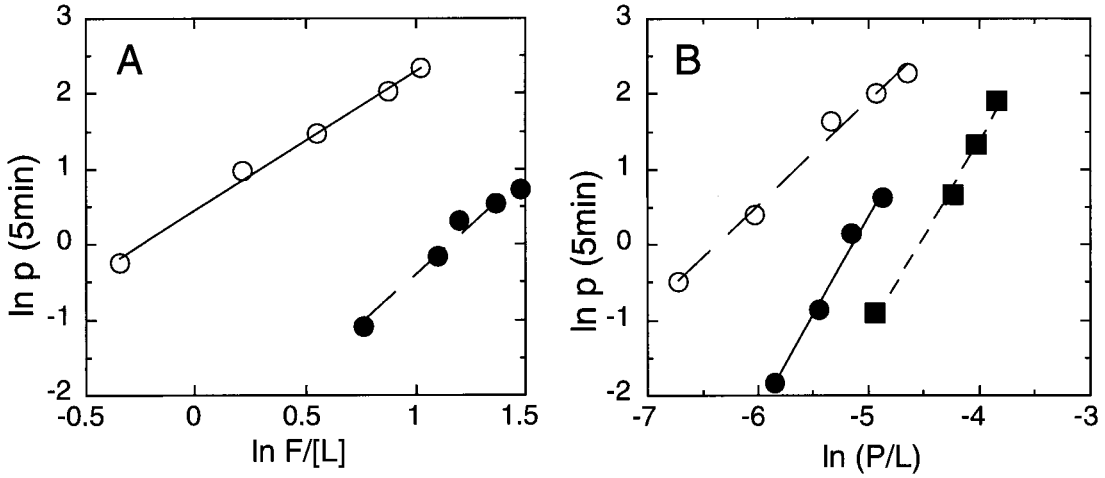

FIGURE 10 Pore molecularity. (*A*) The number of pores formed in 5 min, p, is logarithmically plotted as a function of the ratio of initial dansyl fluorescence intensity-to-lipid concentration obtained from Fig. 7. Peptides: ○, θp100; ●, θp180. The slopes of the regression lines were 1.8 and 2.6, respectively. (*B*) Peptides: ●, F5W-magainin 2 (+3 charge); ■, F12W, E19Q-magainin 2 amide (+5 charge); ○, PGLa (+5 charge). The slopes of the regression lines were 2.6, 2.5, and 1.4, respectively. Data were taken from Matsuzaki et al. (1997a, 1998a).

(FITC-dextran) value of 0.88 was significantly larger than the predicted value of $(0.32)^{1/2} = 0.57$.

Both calcein and ANTS/DPX leakage experiments showed that leakage occurs in a graded manner, suggesting that the pores formed by θp100 and θp180 are short-lived. Fig. 5 *A* indicates that the lifetime τ of θp100 pores was $0.1\tau_0$, whereas that of θp180 pores was $1.2\tau_0$. The above discussion estimated that $1 \leq A_p$ (θp180)/A_p (θp100) = τ_0 (θp100)/τ_0 (θp180) ≤ 4. Therefore, it may be concluded that τ (θp100) < τ (θp180).

θp100 pores were DPX (cation)-selective, whereas θp180 pores were nonselective (Fig. 6), which may be ascribed to the difference in pore size. However, the observation that lipid flip-flop induced by θp100 is faster than that by θp180 at P/L values at which calcein leakage activities were almost the same (Fig. 9) suggested the hypothesis that the wall of the θp100 pores is more negatively charged because of incorporation of larger numbers of lipid molecules. The effects of pore charge on τ_0 are not yet clear.

The finding that FITC-dextran (MW 4400) was permeable across the θp180 pores suggested that peptides (MW ~1900) may also translocate across lipid bilayers through the pores. Nevertheless, the faster translocation of θp100 (Fig. 8) can be explained by faster pore formation and shorter pore lifetime (Fig. 5) because translocation occurs on disintegration of the pore.

In accordance with the results for the model peptides, PGLa, with a polar angle of 100°, exhibited more efficient translocation as well as lipid flip-flop compared with magainin 2, with a polar angle of 180° (Matsuzaki et al., 1998a). Closer inspection of Fig. 7 reveals that the slower binding phase is sigmoidal. Similar behaviors were observed in leakage kinetics (data not shown). A tentative explanation for this is that a time-dependent increase in the amount of membrane-bound peptides changes pore properties.

The hypothesis that the θp100 pores contain more lipid molecules than the θp180 pores despite their smaller size implies that the θp100 pores are composed of a smaller number of peptide molecules, which should be reflected by the dose dependence of pore formation rate. Fig. 10 shows logarithmic plots of the number of pores formed during a 5-min period as a function of the ratio of initial dansyl fluorescence intensity-to-lipid concentration obtained from Fig. 7, which is proportional to the bound peptide-to-lipid ratio. Comparison of the slopes (1.8 versus 2.6) for the two regression lines indicated that the average number of peptides in the θp100 pores was smaller than that in θp180 pores, supporting the above hypothesis.

Fig. 10 *B* shows similar plots for magainins and PGLa, in which the abscissa is P/L (the peptides were completely membrane-bound). The slope (1.4) for PGLa with a polar angle corresponding to that of θp100 was again smaller than that (2.6) of F5W-magainin 2, with a polar angle of 180°. In addition, the slopes for the two magainin 2 analogs with different charges were almost the same, indicating that not the charge density but the polar angle determines the number of peptides per pore. The data also showed that an increase in peptide charge reduces the pore formation rate because of the enhanced electrostatic repulsion.

CONCLUSIONS

Like naturally occurring peptides, simple model peptides also formed peptide-lipid supramolecular pores in PG-based membranes, inducing membrane permeabilization, lipid flip-

flop, and peptide translocation. The pore structure involves negative curvature in the direction perpendicular to the helix axis. Peptides with narrower polar angles more easily deform membranes into this structure. Such peptides form pores composed of fewer peptide molecules and more lipid molecules compared with peptides with a wide polar angle.

This work was supported in part by the Mochida Memorial Foundation for Medical and Pharmaceutical Research, the Kato Memorial Bioscience Foundation, the Mitsubishi Foundation, and the Novartis Foundation (Japan) for the Promotion of Science.

REFERENCES

Bartlett, G. R. 1959. Phosphorus assay in column chromatography. *J. Biol. Chem.* 234:466–468.

Bechinger, B. 1999. The structure, dynamics and orientation of antimicrobial peptides in membranes by multidimensional solid-state NMR spectroscopy. *Biochim. Biophys. Acta.* 1462:157–183.

Blondelle, S. E., and R. A. Houghten. 1992. Design of model amphipathic peptides having potent antimicrobial activities. *Biochemistry.* 31: 12688–12694.

Dathe, M., M. Schümann, T. Wieprecht, A. Winkler, K. Matsuzaki, O. Murase, M. Beyermann, E. Krause, and M. Bienert. 1996. Peptide helicity and membrane surface charge modulate the balance of electrostatic and hydrophobic interactions with lipid bilayers and biological membranes. *Biochemistry.* 35:12612–12622.

Dathe, M., T. Wieprecht, H. Nikolenko, L. Handel, W. L. Maloy, D. L. MacDonald, M. Beyermann, and M. Bienert. 1997. Hydrophobicity, hydrophobic moment and angle subtended by charged residues modulate antibacterial and haemolytic activity of amphipathic helical peptides. *FEBS Lett.* 403:208–212.

Deisenhofer, J., and H. Michel. 1989. The photosynthetic reaction centre from the purple bacterium *Rhodopseudomonas viridis*. *EMBO J.* 8:2149–2170.

Epand, R. M., Y. Shai, J. P. Segrest, and G. M. Anantharamaiah. 1995. Mechanisms for the modulation of membrane bilayer properties by amphipathic helical peptides. *Biopolymers.* 37:319–338.

Fauchere, J.-L., and V. Pliska. 1983. Hydrophobic parameters π of amino-acid side chains from partitioning of N-acetyl-amino-acid amides. *Eur. J. Med. Chem. Chim. Ther.* 18:369–375.

Hancock, R. E. W., T. Falla, and M. H. Brown. 1995. Cationic bactericidal peptides. *Adv. Microb. Physiol.* 37:135–175.

Hancock, R. E. W. 1999. Host defence (cationic) peptides: what is their future clinical potential? *Drugs.* 57:469–473.

Hoffmann, W., K. Richter, and G. Kreil. 1983. A novel peptide designated PYLa and its precursor as predicted from cloned mRNA of *Xenopus laevis* skin. *EMBO J.* 2:711–714.

Javadpour, M. M., and M. M. Juban. 1996. De novo antimicrobial peptides with low mammalian cell toxicity. *J. Med. Chem.* 39:3107–3113.

Ladokhin, A. S., W. C. Wimley, and S. H. White. 1995. Leakage of membrane vesicle contents: determination of mechanism using fluorescence requenching. *Biophys. J.* :1964–1971.

Landolt-Marticorena, C., K. A. Williams, C. M. Deber, and R. A. Reithmeier. 1993. Non-random distribution of amino acids in the transmembrane segments of human type I single span membrane proteins. *J. Mol. Biol.* 229:602–608.

Maloy, W. L., and U. P. Kari. 1995. Structure-activity studies on magainins and other host defense peptides. *Biopolymers.* 37:105–122.

Matsuzaki, K. 1998. Magainins as paradigm for the mode of action of pore forming polypeptides. *Biochim. Biophys. Acta.* 1376:391–400.

Matsuzaki, K. 1999. Why and how are peptide-lipid interactions utilized for self-defense? Magainins and tachyplesins as archetypes. *Biochim. Biophys. Acta.* 1462:1–10.

Matsuzaki, K., M. Harada, S. Funakoshi, N. Fujii, and K. Miyajima. 1991. Physicochemical determinants for the interactions of magainins 1 and 2 with acidic lipid bilayers. *Biochim. Biophys. Acta.* 1063:162–170.

Matsuzaki, K., Y. Mitani, K. Akada, O. Murase, S. Yoneyama, M. Zasloff, and K. Miyajima. 1998a. Mechanism of synergism between antimicrobial peptides magainin 2 and PGLa. *Biochemistry.* 37:15144–15153.

Matsuzaki, K., O. Murase, N. Fujii, and K. Miyajima. 1995a. Translocation of a channel-forming antimicrobial peptide, magainin 2, across lipid bilayers by forming a pore. *Biochemistry.* 34:6521–6526.

Matsuzaki, K., O. Murase, N. Fujii, and K. Miyajima. 1996a. An antimicrobial peptide, magainin 2, induced rapid flip-flop of phospholipids coupled with pore formation and peptide translocation. *Biochemistry.* 35:11361–11368.

Matsuzaki, K., O. Murase, and K. Miyajima. 1995b. Kinetics of pore formation induced by an antimicrobial peptide, magainin 2. *Biochemistry.* 34:12553–12559.

Matsuzaki, K., O. Murase, H. Tokuda, S. Funakoshi, N. Fujii, and K. Miyajima. 1994. Orientational and aggregational states of magainin 2 in phospholipid bilayers. *Biochemistry.* 33:3342–3349.

Matsuzaki, K., S. Nakai, T. Handa, Y. Takaishi, T. Fujita, and K. Miyajima. 1989. Hypelcin A, an α-aminoisobutyric acid containing antibiotic peptide, induced permeability change of phosphatidylcholine bilayers. *Biochemistry.* 28:9392–9398.

Matsuzaki, K., A. Nakamura, O. Murase, K. Sugishita, N. Fujii, and K. Miyajima. 1997a. Modulation of magainin 2-lipid bilayer interactions by peptide charge. *Biochemistry.* 36:2104–2111.

Matsuzaki, K., K. Sugishita, N. Fujii, and K. Miyajima. 1995c. Molecular basis for membrane selectivity of an antimicrobial peptide, magainin 2. *Biochemistry.* 34:3423–3429.

Matsuzaki, K., K. Sugishita, M. Harada, N. Fujii, and M. Miyajima. 1997b. Interactions of an antimicrobial peptide, magainin 2, with outer and inner membranes of gram-negative bacteria. *Biochim. Biophys. Acta.* 1327:119–130.

Matsuzaki, K., K. Sugishita, N. Ishibe, M. Ueha, S. Nakata, M. Miyajima, and R. M. Epand. 1998b. Relationship of membrane curvature to the formation of pores by magainin 2. *Biochemistry.* 37:11856–11863.

Matsuzaki, K., S. Yoneyama, and K. Miyajima. 1997c. Pore formation and translocation of melittin. *Biophys. J.* 73:831–838.

Matsuzaki, K., S. Yoneyama, O. Murase, and K. Miyajima. 1996b. Transbilayer transport of ions and lipids coupled with mastoparan X translocation. *Biochemistry.* 35:8450–8456.

Schwarz, G., and A. Arbuzova. 1995. Pore kinetics reflected in the dequenching of a lipid vesicle entrapped fluorescent dye. *Biochim. Biophys. Acta.* 1239:51–57.

Schwarz, G., and C. H. Robert. 1990. Pore formation kinetics in membranes, determined from the release of marker molecules out of liposomes or cells. *Biophys. J.* 58:577–583.

Takakuwa, T., T. Konno, and H. Meguro. 1985. A new standard substance for calibration of circular dichroism: ammonium *d*-10-camphorsulfonate. *Anal. Sci.* 1:215–218.

Wieprecht, T., M. Dache, and E. Krause. 1997a. Modulation of membrane activity of amphipathic, antibacterial peptides by slight modifications of the hydrophobic moment. *FEBS Lett.* 417:135–140.

Wieprecht, T., M. Dathe, M. Beyermann, E. Krause, W. L. Maloy, D. L. MacDonald, and M. Bienert. 1997b. Peptide hydrophobicity controls the activity and selectivity of magainin 2 amide in interaction with membranes. *Biochemistry.* 36:6124–6132.

Wieprecht, T., M. Dathe, R. M. Epand, M. Beyermann, E. Krause, W. L. Maloy, D. L. MacDonald, and M. Bienert. 1997c. Influence of the angle subtended by the positively charged helix face on the membrane activity of amphipathic, antimicrobial peptides. *Biochemistry.* 36:12869–12880.

Wimley, W. C., M. E. Selsted, and S. H. White. 1994. Interactions between human defensins and lipid bilayers: evidence for formation of multimeric pores. *Protein Sci.* 3:1362–1373.

Zasloff, M. 1987. Magainins, a class of antimicrobial peptides from *Xenopus* skin: isolation, characterization of two active forms, and partial cDNA sequence of a precursor. *Proc. Natl. Acad. Sci. USA.* 84: 5449–5453.